CHEMISTRY
A EUROPEAN JOURNAL

DOI: 10.1002/chem.200701352

Unique Properties of DNA Interstrand Cross-Links of Antitumor Oxaliplatin and the Effect of Chirality of the Carrier Ligand

Jana Kasparkova,[a] Marie Vojtiskova,[a] Giovanni Natile,[b] and Viktor Brabec*[a]

Abstract: The different antitumor and other biological effects of the third-generation antitumor platinum drug oxaliplatin [(1*R*,2*R*-diamminocyclohexane)oxalatoplatinum(II)] in comparison with those of conventional cisplatin [*cis*-diamminedichloridoplatinum(II)] are often explained by the ability of oxaliplatin to form DNA adducts of different conformation and consequently to exhibit different cytotoxic effects. This work describes, for the first time, the structural and biochemical characteristics of the interstrand cross-links of oxaliplatin. We find that: 1) DNA bending, unwinding, thermal destabilization, and delocalization of the conformational alteration induced by the cross-link of oxaliplatin are greater than those observed with the cross-link of cisplatin; 2) the affinity of high-mobility-group proteins (which are known to mediate the antitumor activity of platinum complexes) for the interstrand cross-links of oxaliplatin is markedly lower than for those of cisplatin; and 3) the chirality at the carrier 1,2-diaminocyclohexane ligand can affect some important structural properties of the interstrand cross-links of cisplatin analogues. Thus, the information contained in the present work is also useful for a better understanding of how the stereochemistry of the carrier amine ligands of cisplatin analogues can modulate their anticancer and mutagenic properties. The significance of this study is also reinforced by the fact that, in general, interstrand cross-links formed by various compounds of biological significance result in greater cytotoxicity than is expected for monofunctional adducts or other intrastrand DNA lesions. Therefore, we suggest that the unique properties of the interstrand cross-links of oxaliplatin are at least partly responsible for this drug's unique antitumor effects.

Keywords: antitumor agents · conformation analysis · DNA · platinum · structure–activity relationships

Introduction

Oxaliplatin [(1*R*,2*R*-diamminocyclohexane)oxalatoplatinum-(II)] (Scheme 1) is a third-generation platinum antitumor compound. It is a drug in the same family as cisplatin [*cis*-diamminedichloridoplatinum(II)] and carboplatin [*cis*-diammine-cyclobutanedicarboxylatoplatinum(II)]. It is typically administered in combination with fluorouracil and leucovorin for the treatment of colorectal cancer.[1] In relation to cisplatin, the two amine groups are replaced by cyclohexanediamine for improved antitumor activity. The chlorido ligands are replaced by the bidentate oxalato group derived from oxalic acid in order to improve water solubility.

The cytotoxicity of platinum compounds is thought to result primarily from the formation of DNA–platinum intrastrand and interstrand cross-links (CLs), but the relative efficacy of these CLs remains unknown.[2,3] The sequence and

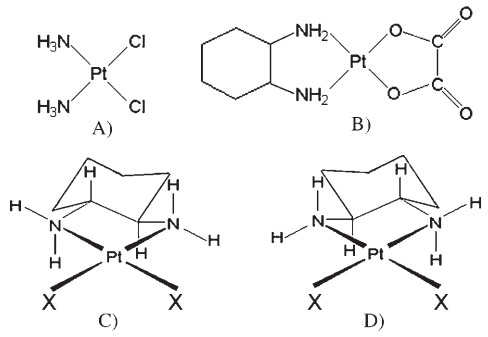

Scheme 1. Structures of platinum compounds: A) cisplatin, B) oxaliplatin, C) $[Pt(R,R\text{-dach})]^{2+}$, and D) $[Pt(S,S\text{-dach})]^{2+}$.

[a] Dr. J. Kasparkova, Dr. M. Vojtiskova, Prof. Dr. V. Brabec
Institute of Biophysics
Academy of Sciences of the Czech Republic, v.v.i.
Kralovopolska 135, 61265 Brno (Czech Republic)
Fax: (+42) 541-240-499
E-mail: brabec@ibp.cz

[b] Prof. Dr. G. Natile
Department of Pharmaceutical Chemistry
University of Bari, 70125 Bari (Italy)

region specificity and the type and frequency of adducts formed by oxaliplatin and cisplatin appear to be similar.[4–6] Thus, oxaliplatin would be expected to damage DNA to a similar extent as cisplatin. However, various methodologies have suggested that oxaliplatin induces fewer lesions in naked and cellular DNA than equimolar cisplatin does.[6–8] These findings suggest that oxaliplatin-induced DNA damage may differ in various aspects from that of cisplatin. Recently, structural differences between 1,2-GG intrastrand CLs (G: guanine) of oxaliplatin and cisplatin have been suggested to explain some of the differences between the biological effects of these two platinum drugs.[9–11] An intriguing, but so far not examined, eventuality is that oxaliplatin cytotoxicity might possibly result from relatively more lethal lesions, such as interstrand CLs. Hence, it is of particular interest to shed light on the distortions induced in DNA by interstrand CLs of oxaliplatin.

The determination of the structure of these CLs is a key step which may give a new insight into the formation, stability, cellular processing, and repair of oxaliplatin lesions. In order for the reaction of oxaliplatin with DNA to occur, the parent compound must become aquated. The hydrolysis of oxaliplatin to form the reactive diaqua species [Pt(*R*,*R*-dach)$(H_2O)_2]^{2+}$ (dach: 1,2-diaminocyclohexane; Scheme 1) is a slower process than the hydrolysis of cisplatin. In addition, besides oxaliplatin, another enantiomeric form of this complex exists, so a comparison of the effects of interstrand CLs of platinum complexes with enantiomeric amine ligands, such as $[Pt(R,R\text{-dach})]^{2+}$ (derived from oxaliplatin) and $[Pt(S,S\text{-dach})]^{2+}$, on DNA conformation is also of great interest. To achieve this, various biochemical methods that are currently used for characterization of DNA distortion induced by DNA-damaging agents were employed in the present work to characterize the interstrand CLs of $[Pt(R,R\text{-dach})]^{2+}$ and its *S*,*S* enantiomer. In addition, the recognition and binding of various proteins have been shown to play an important role in the mechanism of antitumor effects of platinum antitumor drugs, with abundant high-mobility-group (HMG) domain proteins binding to platinated DNA being most frequently studied.[12] Hence, recognition by HMGB1 domain proteins of DNA duplexes containing single, site-specific interstrand CLs of $[Pt(R,R\text{-dach})]^{2+}$ (oxaliplatin) and $[Pt(S,S\text{-dach})]^{2+}$ was also assayed. The results are compared with the data obtained previously or in the present work for the interstrand CL of cisplatin.

Results

Frequency of interstrand cross-links and preferential sites involved in these adducts: It has already been shown that the sites in DNA and the spectra of oxaliplatin adducts are nearly identical to those in the situation in which DNA is modified by cisplatin.[6] Therefore, we decided to confirm that the reactive form of oxaliplatin produces the interstrand CLs with the same rate and in the sequence in which cisplatin preferentially forms interstrand CLs, that is, between guanine residues in the sequence 5′-GC/5′-GC (C: cytosine).[13]

We quantitated the interstrand cross-linking efficiency of $[Pt(R,R\text{-dach})]^{2+}$, $[Pt(S,S\text{-dach})]^{2+}$, and cisplatin in a 2455-bp DNA fragment, which was modified by these complexes at 37 °C for 24 h so that a value of $r_b = 0.001$ was attained (r_b is defined as the amount of platinum atoms bound per one nucleotide in DNA). The samples were analyzed for the interstrand CLs by agarose gel electrophoresis under denaturing conditions, as described in the Experimental Section. Upon electrophoresis, 3′-end-labeled strands of the 2455-bp DNA migrate as a 2455-mer single strand, whereas the interstrand cross-linked strands migrate more slowly as a higher molecular mass species (Figure 1). The bands corresponding

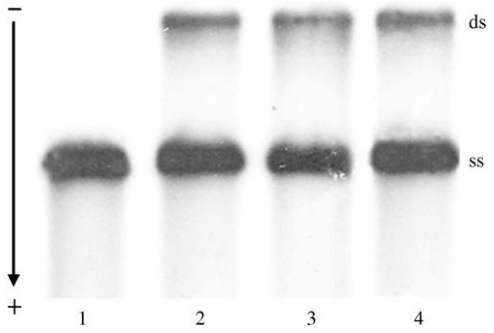

Figure 1. The formation of the interstrand CLs by platinum complexes in the linear pSP73KB plasmid (2455 bp). Autoradiogram of denaturing 1% agarose gel of the DNA fragments that were 3′-end labeled. The interstrand cross-linked DNA appears as the top band, which is migrating on the gel more slowly than the single-stranded DNA (contained in the bottom band). The DNA fragments were nonplatinated (control; lane 1) or incubated for 24 h with $[Pt(R,R\text{-dach})]^{2+}$ (oxaliplatin), $[Pt(S,S\text{-dach})]^{2+}$, or cisplatin (lanes 2–4, respectively). The r_b value was 0.001.

to the more slowly migrating interstrand cross-linked fragments (2455 nucleotides) were seen for both enantiomers (Figure 1, lanes 2 and 3). The intensity of these more slowly migrating bands corresponding to the interstrand-cross-linked fractions was the same for both enantiomers. The frequencies of interstrand CLs of $[Pt(R,R\text{-dach})]^{2+}$ and $[Pt(S,S\text{-dach})]^{2+}$ (the number of interstrand CLs per adduct) were 5.7 ± 0.4 and 5.5 ± 0.5%, that is, these frequencies were very similar to that found for cisplatin (5.5 ± 0.3%).

Cisplatin and its bifunctional analogues react with DNA in a two-step process.[14] Monofunctional adducts are formed preferentially at the N7 atoms of G residues. These lesions subsequently close to bifunctional CLs (intrastrand and/or interstrand). By considering this fact, we have designed the synthetic oligodeoxyribonucleotide duplex TCGCT (shown in Figure 2C, containing a central TCGCT sequence in the pyrimidine-rich top strand and a central AGCGA sequence in the complementary bottom strand; the top and bottom strands of each pair of duplexes used in the present work are designated 'top' and 'bottom', respectively, throughout). The pyrimidine-rich top strand of this duplex contains a

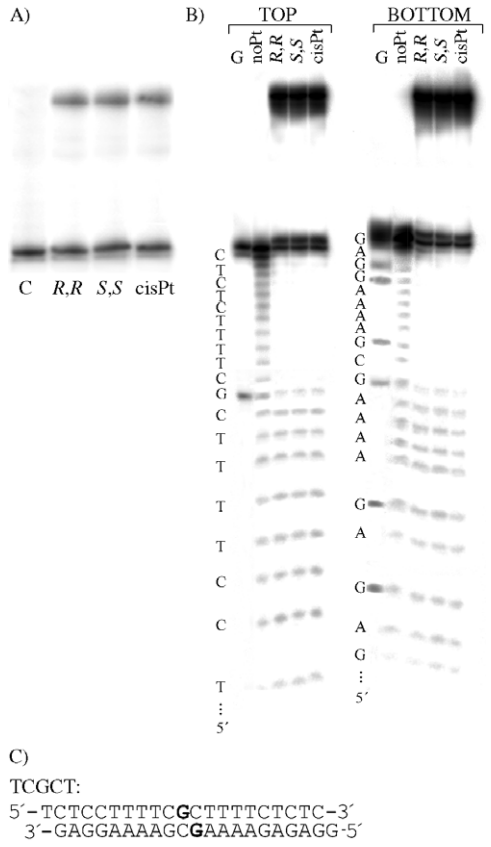

Figure 2. The interstrand cross-link formation in the oligodeoxyribonucleotide duplex (TCGCT shown in C) formed at 37 °C by mixing the top strand uniquely monoadducted by $[Pt(R,R\text{-dach})]^{2+}$ (oxaliplatin), $[Pt(S,S\text{-dach})]^{2+}$, or cisplatin at the central G residue with the bottom strand. A) Autoradiogram of a 12% PAA/urea denaturing gel of the duplexes the bottom strand of which was 5′-end labeled. The cross-linking reaction was stopped after 24 h by adjusting the NaOH concentration to 10 mM and cooling the samples to 0 °C. Lanes: C: control, unmodified duplex; *R*,*R*, *S*,*S*, cisPt: duplex cross-linked by $[Pt(R,R\text{-dach})]^{2+}$, $[Pt(S,S\text{-dach})]^{2+}$, or cisplatin, respectively. B) Hydroxyl-radical footprinting of interstrand cross-links of $[Pt(R,R\text{-dach})]^{2+}$, $[Pt(S,S\text{-dach})]^{2+}$, or cisplatin. Shown are autoradiograms of the denaturing 24% PAA/8 M urea gel of the products of the reaction between hydroxyl radicals and the duplex TCGCT either unmodified or containing an interstrand CL. The top (left) or bottom (right) strand was 5′-end labeled. Lanes: noPt: unplatinated duplex; *R*,*R*, *S*,*S*, cisPt: duplex containing an interstrand CL of $[Pt(R,R\text{-dach})]^{2+}$, $[Pt(S,S\text{-dach})]^{2+}$, or cisplatin, respectively; G: a Maxam–Gilbert specific reaction for the unplatinated duplex. For further details, see the text. C) Sequence and abbreviation of the synthetic oligodeoxyribonucleotide duplex used for analysis of interstrand cross-links. The boldface letters indicate the platinated residues in the interstrand cross-linked duplexes.

unique G residue, at which the monofunctional adduct of $[Pt(R,R\text{-dach})]^{2+}$, $[Pt(S,S\text{-dach})]^{2+}$, or cisplatin was formed. Thus, the choice of this oligonucleotide allowed for a cross-linking study under competitive conditions (that is, three types of interstrand CLs were in principle possible: between the central G residue in the top strand and the complementary C residue or the 5′- or 3′-G residues adjacent to the complementary C residue in the bottom strand).

The top strands of the duplexes containing the monofunctional adducts of $[Pt(R,R\text{-dach})]^{2+}$, $[Pt(S,S\text{-dach})]^{2+}$, or cisplatin were hybridized with the complementary (bottom) strand which was ^{32}P-labeled at the 5′ end. The mixtures were incubated at 37 °C in $NaClO_4$ (0.1 M) for 48 h and subjected to gel electrophoresis under denaturing (strand-separating) conditions to detach the two strands of the duplexes. A new band migrating more slowly and corresponding to two cross-linked strands was clearly seen (Figure 2A). The yields of these interstrand cross-linking reactions were approximately 40% for both enantiomers and cisplatin. It was verified that, after the treatment of the species contained in the more slowly migrating band with NaCN (0.2 M, pH 11), the product migrated in the gel as a single strand (not shown).

The interstrand cross-linked samples (the bands corresponding to the interstrand cross-linked duplexes were cut off and the duplexes were eluted and purified by standard procedures) were further analyzed by hydroxyl-radical footprinting.[15,16] The hydroxyl radicals generated by reaction of the ethylenediaminetetraacetate (EDTA) complex of iron(II) with hydrogen peroxide initiate cleavage of the DNA phosphodiester backbone by abstracting a hydrogen atom from a deoxyribose. The key experimental advantage of the hydroxyl radical as a chemical probe is that it effects DNA cleavage with no base or sequence specificity. We used hydroxyl-radical footprinting to identify the nature of the bases in the duplexes interstrand cross-linked by $[Pt(R,R\text{-dach})]^{2+}$, $[Pt(S,S\text{-dach})]^{2+}$, or cisplatin. These duplexes containing a single interstrand CL were ^{32}P-labeled at the 5′ end of either the pyrimidine-rich strand or the purine-rich strand. The fragments generated by hydroxyl radicals were separated on a polyacrylamide (PAA) gel under denaturing conditions. The cleavage patterns for the platinated and unplatinated oligonucleotides, as well as the Maxam–Gilbert sequencing patterns for the unplatinated oligonucleotides (a guanine-specific reaction making it possible to identify the location of guanine residues in each strand), are shown in Figure 2B. For the two strands of the unplatinated duplex, a uniform cleavage was obtained (Figure 2B, lane noPt). For the platinated duplexes, all of the bases from the 5′ end up to the interstrand CL were detected. All of the other bases were undetected because the generated fragments were cross-linked and consequently migrated with a reduced mobility compared to that of each unplatinated strand.

Thus, from the observation that all fragments corresponding to cleavage by hydroxyl radicals from the 5′ end up to the interstrand CL were detected and separated according to size on a PAA gel (Figure 2B), the exact location of the bases involved in the interstrand CL was deduced.[15,16] The interstrand CLs formed by $[Pt(R,R\text{-dach})]^{2+}$, $[Pt(S,S\text{-dach})]^{2+}$, and cisplatin in the duplex TCGCT were unambiguously identified as 1,2-GG interstrand adducts involving the central G site in the top strand and the G residue of the neighboring base pair in the bottom strand (Figure 2B), that is, between G residues in the 5′-GC/5′-GC sequence. Thus, these results are consistent with the hypothesis that both $[Pt(R,R\text{-dach})]^{2+}$ and $[Pt(S,S\text{-dach})]^{2+}$ readily form interstrand CLs in the 5′-GC/5′-GC sequence like cisplatin.

Conformational changes produced in double-helical DNA by the site-specific interstrand cross-link: In contrast to cisplatin, oxaliplatin forms DNA adducts that contain the *R*,*R*-DACH carrier ligand. The goal of this work was to establish whether the steric structure of the nonleaving group of platinum DACH enantiomers affects distortions induced in DNA by the formation of the interstrand CLs. We have analyzed oligodeoxyribonucleotide duplexes containing a single, site-specific interstrand CL of $[Pt(R,R\text{-dach})]^{2+}$, $[Pt(S,S\text{-dach})]^{2+}$, or cisplatin by using various biochemical and biophysical methods, such as measurements of DNA melting, CD spectroscopy, chemical probing of DNA conformation, and electrophoretic retardation as a quantitative measure of local bending and unwinding.

DNA melting: Melting-temperature measurements by UV absorption spectrophotometry were conducted to characterize the thermally induced denaturation of the 15-bp duplex TGCT(15) (see Figure 3A for the sequence) with the specific goal of elucidating the thermal consequences of modifying and constraining DNA through a single, site-specific interstrand CL of $[Pt(R,R\text{-dach})]^{2+}$, $[Pt(S,S\text{-dach})]^{2+}$, or cisplatin. The CLs were formed in the center of these duplexes between G residues in the 5′-GC/5′-GC sequence. Comparison of the melting temperatures (T_m) for the cross-linked duplexes and for the unconstrained (unplatinated) duplex (Table 1) reveals that formation of either CL results in a substantial increase in the thermal stability of the duplex (the differences between the T_m values of the cross-linked and unplatined parental duplex, ΔT_m, were 20.8, 22.4, or 18.2 °C for the CLs of $[Pt(R,R\text{-dach})]^{2+}$, $[Pt(S,S\text{-dach})]^{2+}$, and cisplatin, respectively).

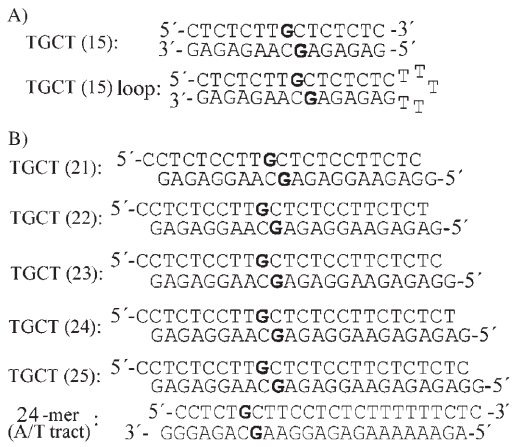

Figure 3. Nucleotide sequences of the synthetic oligodeoxyribonucleotides. A) Sequences of the oligonucleotides used in DNA melting experiments. B) Sequences of the oligonucleotides used in DNA bending and unwinding experiments and their abbreviations. The boldface letters indicate the platinated residues in the interstrand cross-linked duplexes.

Table 1. Melting temperatures, T_m, of duplexes that were unplatinated or contained a single, site-specific interstrand cross-link of $[Pt(R,R\text{-dach})]^{2+}$, $[Pt(S,S\text{-dach})]^{2+}$, or cisplatin.

Duplex	T_m [°C][a]
TGCT(15)-noPt[b]	51.2
TGCT(15)-loop (noPt)[c]	75.4
TGCT(15)-*R*,*R*[d]	72.0
TGCT(15)-*S*,*S*[e]	73.6
TGCT(15)-cisPt[f]	69.4

[a] The error is ±0.3 °C. [b] Unplatinated duplex TGCT(15). [c] Unplatinated hairpin duplex; the stem duplex of this hairpin structure contained two complementary nucleotide sequences identical to those of the top and bottom strands of the duplex TGCT(15), which were linked in this duplex by a short single-stranded loop composed of five thymine residues. [d] Duplex TGCT(15) containing a cross-link of $[Pt(R,R\text{-dach})]^{2+}$. [e] Duplex TGCT(15) containing a cross-link of $[Pt(S,S\text{-dach})]^{2+}$. [f] Duplex TGCT(15) containing a cross-link of cisplatin.

The unconstrained (unplatinated) duplex TGCT(15) denatures in a bimolecular reaction to form two single strands. As a consequence, the melting of the unplatinated duplex was dependent on the overall oligonucleotide concentration. By contrast, the duplexes containing the interstrand CL melted in a concentration-independent manner to a denatured state, which is consistent with the expectation that the molecularity had been reduced from bimolecular to monomolecular due to the presence of the interstrand CL. Thus, the observed ΔT_m values are apparently affected by the fact that the original bimolecular oligomer system became monomolecular as a consequence of the cross-linking. Upon introduction of a single platinum interstrand CL, the change in the T_m value can result not only from the change in the molecularity of the system but also from a different mechanism for the melting transition. We tried to dissect these two components of the observed cross-link-induced shift in thermal stability. To estimate how much of the observed ΔT_m difference results from the change in molecularity, we used an approach based on examination of the thermal transition of the hairpin (duplex TGCT(15) loop, Figure 3A). The stem duplex of this hairpin structure contained two complementary nucleotide sequences identical to those of the top and bottom strands of duplex TGCT(15); however, these strands were still linked by a short single-stranded loop composed of five thymine residues. The thymine residues in this short loop behave as denatured single strands and should contribute little to the transition energetics of an adjacent stem duplex.[17,18] Hence, it is reasonable to expect that the hairpin TGCT(15) loop melts in the same way as the duplex TGCT(15) but in a monomolecular, concentration-independent reaction.[18] In this way, if the ΔT_m value is calculated as the difference between the values of T_m for the interstrand cross-linked duplex TGCT(15) and the nonplatinated hairpin TGCT(15) loop, one "corrects" for the concentration dependence of the T_m value of duplex TGCT(15) and obtains the change in the T_m value corresponding to effects other than the change in molecularity of the system.

Examination of the thermal melting of the nonmodified hairpin TGCT(15) loop revealed that its melting temperature was 75.4 °C, that is, a value 24.2 °C higher than that found for duplex TGCT(15). Hence, this value can be taken in the first approximation as a "reduced" concentration-in-

dependent melting temperature for the nonmodified duplex TGCT(15). This "reduced" T_m value of the unplatinated duplex is significantly different from the T_m values of the cross-linked duplexes. Formation of the interstrand CL in DNA by [Pt(*R*,*R*-dach)]$^{2+}$, [Pt(*S*,*S*-dach)]$^{2+}$, or cisplatin decreased the thermal stability of DNA, with the CL of cisplatin being most efficient and that of [Pt(*S*,*S*-dach)]$^{2+}$ being least efficient (Table 2). Hence, the overall impact of a single interstrand CL of [Pt(*R*,*R*-dach)]$^{2+}$, [Pt(*S*,*S*-dach)]$^{2+}$, or cisplatin should not be associated only with the change in molecularity of the duplex system; instead, another mechanism also has to be involved in lowering the thermal stability of the duplex,[19] presumably through conformational alterations.

Table 2. Summary of the results demonstrating the properties of interstrand cross-links formed by [Pt(*R*,*R*-dach)]$^{2+}$ (oxaliplatin), [Pt(*S*,*S*-dach)]$^{2+}$, and cisplatin in the 5′-GC/5′-GC sequence.

Interstrand CL of:	ΔT_m [°C][a]	Bending [°][b]	Unwinding [°]	Chemical probes[d]	Recognition by: HMGB1a	HMGB1b
cisplatin	6.0 ± 0.2	45 ± 2[c]	79 ± 3[c]	TTGCT AACGA	no[e]	yes[e]
[Pt(*R*,*R*-dach)]$^{2+}$	3.4 ± 0.2	56 ± 2	96 ± 2	TTGCT AACGA	no	no
[Pt(*S*,*S*-dach)]$^{2+}$	1.8 ± 0.2	61 ± 3	82 ± 1	TTGCT AACGA	no	no

[a] $\Delta T_m = T_m$ (platinated) − T_m (unplatinated); the T_m (unplatinated) value was that found for the unplatinated duplex TGCT(15)-loop, while the T_m (platinated) value was that found for the platinated duplex TGCT(15). The values are "corrected" for the concentration dependence of the T_m value of duplex TGCT(15). See the text for further details. Each value represents the mean value from three melting experiments ± the standard deviation. [b] Toward the minor groove. Each value represents the mean value from three experiments ± the standard deviation. [c] Values from Malinge et al.[28] and the present work. Each value represents the mean value from three independent determinations ± the standard deviation. [d] Summary of the reactivity of chemical probes with the duplexes TGCT containing an interstrand CL formed by cisplatin, [Pt(*R*,*R*-dach)]$^{2+}$, or [Pt(*S*,*S*-dach)]$^{2+}$. Closed and open circles designate strong and weak reactivities, respectively. [e] Values from the present work and that of Kasparkova et al.[32]

Circular dichroism spectroscopy: The CD spectra of the 15-bp duplex TGCT(15) (shown in Figure 4B) containing a single, site-specific interstrand CL of [Pt(*R*,*R*-dach)]$^{2+}$, [Pt(*S*,*S*-dach)]$^{2+}$, or cisplatin and its nonmodified counterpart at 25 °C were also measured to study the macroscopic helical geometry of the nonmodified and cross-linked duplexes and to monitor differences in the overall structures of these duplexes. The perturbation of the B conformation of DNA due to the formation of the interstrand CLs of the three platinum compounds results in the marked red shift of the positive band of DNA at 276 nm and the negative band at 245 nm (Figure 4A). In addition, the intensity of these bands is markedly decreased. Interestingly, the spectra of the duplexes containing the interstrand CLs of [Pt(dach)]$^{2+}$ complexes were different from that of the duplex containing the CL of cisplatin, thereby demonstrating that the interstrand CLs of [Pt(dach)]$^{2+}$ complexes distort the DNA conformation differently to the CLs of cisplatin. Also interestingly, the CD spectra of the duplexes containing the interstrand CLs of [Pt(*R*,*R*-dach)]$^{2+}$ and [Pt(*S*,*S*-dach)]$^{2+}$ differ as well, a fact suggesting a chirality-dependent character of the conformational distortion induced in DNA by interstrand CLs of [Pt(dach)]$^{2+}$ complexes.

Chemical probes: To further characterize the distortions induced in DNA by interstrand CLs of [Pt(*R*,*R*-dach)]$^{2+}$ or [Pt(*S*,*S*-dach)]$^{2+}$, the 23-bp oligonucleotide duplex TGCT(24) (shown in Figure 3B), containing the site-specific interstrand CL of [Pt(*R*,*R*-dach)]$^{2+}$, [Pt(*S*,*S*-dach)]$^{2+}$ or, for comparative purposes, of cisplatin was treated with several chemical agents that are used as tools for monitoring the existence of conformations other than canonical B-DNA. These agents included $KMnO_4$, bromine, or diethyl pyrocarbonate (DEPC) as probes for thymine, cytosine, and ade-

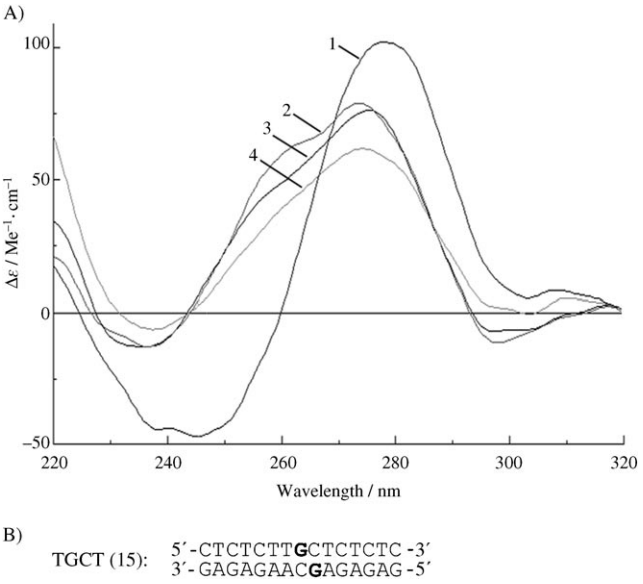

Figure 4. A) CD spectra for the 15-bp duplex (TGCT(15) in B) unplatinated or containing a single, site-specific interstrand cross-link of [Pt(*R*,*R*-dach)]$^{2+}$ (oxaliplatin), [Pt(*S*,*S*-dach)]$^{2+}$, or cisplatin recorded at 25 °C. The duplex concentration was 2 μM and the buffer conditions were tris(hydroxymethyl)aminomethane–HCl (Tris-HCl; 10 mM, pH 7.2), NaCl (0.1 M), and EDTA (0.1 mM). Curves: 1: unplatinated duplex; 2–4: the duplex cross-linked by [Pt(*R*,*R*-dach)]$^{2+}$, [Pt(*S*,*S*-dach)]$^{2+}$, or cisplatin, respectively. B) Sequence and abbreviation of the synthetic oligodeoxyribonucleotide duplex used for analysis by CD spectroscopy. The boldface letters indicate the platinated residues in the interstrand cross-linked duplexes.

nine/guanine residues, respectively.[20–24] These probes react, under the conditions used, with base residues in single-stranded DNA and distorted double-stranded DNA but not with the base residues in intact, double-stranded DNA.[20–24] For this analysis, we used exactly the same methodology as in our recent studies dealing with DNA adducts of various antitumor platinum drugs. Thus, the details of this experiment can be found in those articles[21,25,26] and representative gels showing piperidine-induced specific strand cleavage at $KMnO_4$-modified, $KBr/KHSO_5$-modified, and DEPC-modified bases in the 23-bp duplexes that were unplatinated or contained a single, interstrand CL of $[Pt(R,R\text{-dach})]^{2+}$, $[Pt(S,S\text{-dach})]^{2+}$, or cisplatin are demonstrated in Figure 5. The results are schematically summarized in Table 2.

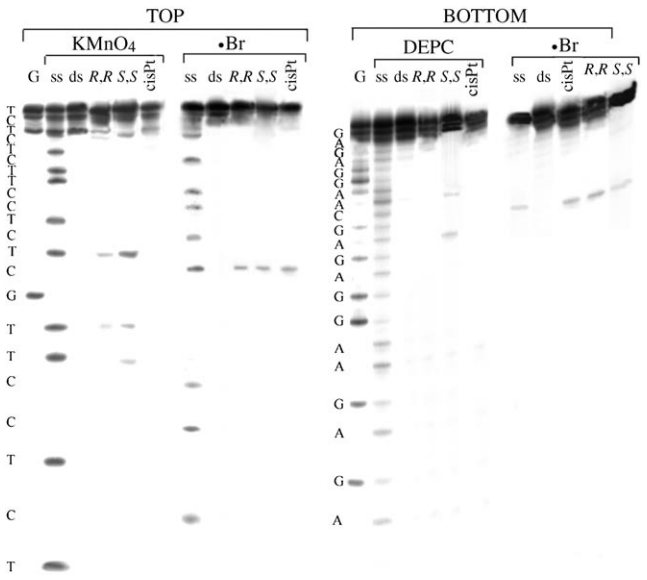

Figure 5. Chemical probes of DNA conformation. Piperidine-induced specific-strand cleavage at $KMnO_4$-modified, $KBr/KHSO_5$-modified, and DEPC-modified bases in the TGCT(24) duplex (shown in Figure 3B) unplatinated or containing a single, site-specific interstrand cross-link of $[Pt(R,R\text{-dach})]^{2+}$ (oxaliplatin), $[Pt(S,S\text{-dach})]^{2+}$, or cisplatin. Lanes: ss: the unplatinated strand; ds: the unplatinated duplex; *R,R*, *S,S*, cisPt: the duplex containing a unique interstrand adduct of $[Pt(R,R\text{-dach})]^{2+}$, $[Pt(S,S\text{-dach})]^{2+}$, or cisplatin, respectively; G: a Maxam–Gilbert specific reaction for the unplatinated duplex. The oligomers were 5′-end labeled on either the top (left panel, marked TOP) or bottom strand (right panel, marked BOTTOM).

The pattern and degree of reactivity toward the chemical probes were similar for the interstrand CLs formed by $[Pt(dach)]^{2+}$ and cisplatin, in that cytosine residues complementary to the guanines modified by these complexes were largely exposed to the solvent (Figure 5 and Table 2). The flanking adenines and thymines were not reactive with DEPC and $KMnO_4$, respectively, in the case of the interstrand CL of cisplatin, a fact indicating that the distortion induced by the formation of this CL was largely localized at the platinated 5′-GC/5′-CG base pairs and no marked local distortion took place in the vicinity of the platination site. This result is in accordance with the previous observation demonstrating that hyperreactivity of the two cytosine residues complementary to the platinated guanines to hydroxylamine and that the distortion is limited to the platinated base pairs.[27] By contrast, the pattern and degree of reactivity toward the chemical probes was different for the interstrand CLs of the two Pt-DACH enantiomers (Figure 5 and Table 2). Few bases flanking the 5′-GC/5′-GC sequence cross-linked by $[Pt(dach)]^{2+}$ compounds were reactive with chemical probes, thereby indicating a different character of the conformational distortion induced in DNA by the interstrand CLs of these compounds. These results suggest that the conformational distortion induced by $[Pt(dach)]^{2+}$ compounds is, in contrast to that with the CL of cisplatin, more delocalized and extends over at least four or five base pairs around the CL. The distortion induced by the interstrand CL of $[Pt(S,S\text{-dach})]^{2+}$ appears to be somewhat more delocalized than that of $[Pt(R,R\text{-dach})]^{2+}$, thereby confirming a chirality-dependent character of the conformational distortion induced in DNA by interstrand CLs of $[Pt(dach)]^{2+}$ complexes.

Bending and unwinding: Among the alterations of the secondary and tertiary structure of DNA to which it may be subject, the role of the intrinsic bending and unwinding of DNA is increasingly recognized as being potentially important in regulating replication and transcription functions through specific DNA–protein interactions. For cisplatin interstrand adducts, the structural details responsible for bending and subsequent protein recognition have been elucidated.[28–32] Given the recent advances in our understanding of the structural basis for the bending of DNA caused by cisplatin, it is also of considerable interest to examine how the character of a carrier amine in the 1,2-GG interstrand adduct affects the conformational properties of DNA, such as bending and unwinding. In this work we further performed studies on the bending and unwinding induced by single, site-specific interstrand CLs of $[Pt(dach)]^{2+}$ enantiomers formed in oligodeoxyribonucleotide duplexes between guanine residues in the 5′-GC/5′-GC sequence.

As in the previous study,[28] we used electrophoretic retardation as a quantitative measure of the extent of planar curvature to analyze the bending and unwinding induced by the single, site-specific interstrand CL formed by $[Pt(R,R\text{-dach})]^{2+}$ or $[Pt(S,S\text{-dach})]^{2+}$. The oligodeoxyribonucleotide duplexes TGCT(21–25) (the sequences of which are shown in Figure 3B) were used in these studies. The ligation products of these unplatinated or [Pt(dach)]-containing duplexes were analyzed on a native PAA electrophoresis gel. Experimental details of these studies have been given in recent reports.[28,33] Importantly, in the present work, we used the oligonucleotide duplexes which had the same nucleotide sequences as those used previously by other authors[28] who analyzed the bending and unwinding induced by the single, site-specific interstrand CL of cisplatin. In addition, we used methodology and experimental conditions in these experiments which were exactly the same as in the previous paper,[28] and we confirmed the previously obtained results that the interstrand CL of cisplatin bent DNA toward the

minor groove by 45° and unwound DNA by 79° (the gel is not shown). Representative gels and the analysis showing the mobility of the ligation products of 21–25-bp duplexes containing single, site-specific, interstrand CLs of [Pt(*R*,*R*-dach)]$^{2+}$ or [Pt(*S*,*S*-dach)]$^{2+}$ at the sequence 5′-GC/5′-GC in a PAA gel are shown in Figure 6A. The results are summarized in Table 2. The DNA bending of 56 and 61° toward the minor groove and the unwinding of 96 and 82° due to the single, site-specific interstrand CLs formed by [Pt(*R*,*R*-dach)]$^{2+}$ or [Pt(*S*,*S*-dach)]$^{2+}$, respectively, indicate that these parameters are different for the two enantiomers and markedly different from those found for the interstrand CL of cisplatin (Table 2). The direction of the bend was determined by using the duplex 24-mer TGCT (A/T tract) (the sequence is shown in Figure 3B), which also contained, besides the single interstrand CL formed by the Pt–DACH enantiomer, the $(A–T)_6$ tract located "in phase" from the CL (the cross-linked base pairs and the center of the A tract were separated by 11 bp), in the same way as in our recent articles.[26,34,35]

The mobility of a linear DNA molecule through a native PAA gel is directly proportional to its end-to-end distance. DNA multimers of identical length and number of bend units, but with differently phased bends, have different end-to-end distances. The DNA bends must be spaced evenly and phased with the DNA helical repeat in order to add constructively. Such constructively phased bends add in plane to yield short end-to-end distances and the most anomalous gel migration. If the ends come close enough together, they may close covalently upon reaction with DNA ligase to form small DNA circles. Produced in ligations of monomers investigated in this work were also some separate bands arising from these small DNA circles, which migrate close to the top of the gel (see the bands marked by asterisks in Figure 6A as an example). The occurrence of small DNA circles was also evident if the platinum was removed from the products of the ligation reaction by NaCN (0.2 M, pH 11)[21] (not shown). The highest tendency to yield DNA circles was observed for the 23- or 24-bp multimers, a fact confirming a close match between the 23- and 24-bp sequence repeats and the helix screw.[21,36,37]

Recognition by HMG domain proteins: An important feature of the mechanism of action of cisplatin is that the bending of the helix axis induced in DNA by 1,2-intrastrand or 1,2-interstrand CLs of cisplatin and the altered structures attract HMG domain proteins and other proteins.[3,12,30,38,39] This binding of HMG domain proteins to DNA modified by cisplatin has been postulated to mediate its antitumor properties.[12,40] Interestingly, full-length HMGB1 or HMGB2 proteins and the domains A and B of the HMGB1 protein (HMGB1a and HMGB1b, respectively) bind to 1,2-GG intrastrand CLs of cisplatin. Even more interestingly, the full-length HMGB1 protein and its domain B, with a lysine-rich region (seven amino acid residues) of the A/B linker attached to its N terminus, specifically recognize DNA that has been interstrand cross-linked by cisplatin.[30,32]

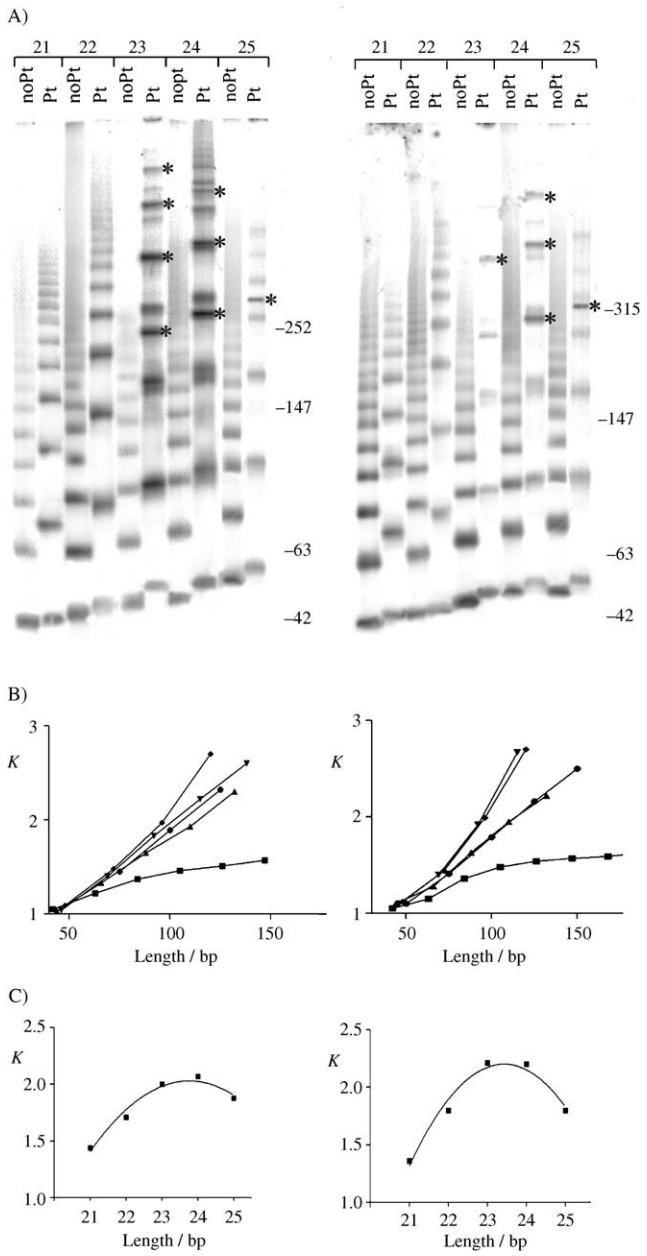

Figure 6. The mobility of the ligation products of 21–25-bp duplexes (TGCT(21–25) shown in Figure 3B) containing a single, site-specific interstrand cross-link of [Pt(*R*,*R*-dach)]$^{2+}$ or [Pt(*S*,*S*-dach)]$^{2+}$ at the central sequence 5′-TGCT/5′-AGCA in an 8% PAA gel. A) Phosphorimage of the ligation products of the duplexes containing an interstrand cross-link of [Pt(*R*,*R*-dach)]$^{2+}$ (left panel) or [Pt(*S*,*S*-dach)]$^{2+}$ (right panel). Lanes: No Pt: unplatinated duplexes; Pt: duplex containing the cross-link. B) Plots showing the relative mobility *K* versus sequence length for the 21–25-bp oligomers containing the CL of [Pt(*R*,*R*-dach)]$^{2+}$ (left) or [Pt(*S*,*S*-dach)]$^{2+}$ (right). Symbols: ■: 21-mer; ▲: 22-mer; ▼: 23-mer; ◆: 24-mer; ●: 25-mer. C) Plots showing the relative mobility *K* versus interadduct distance in bp for the 21–25-bp oligomers containing the CL of [Pt(*R*,*R*-dach)]$^{2+}$ (left) or [Pt(*S*,*S*-dach)]$^{2+}$ (right) with a total length of 100 bp. The experimental points represent the average of three independent experiments. The curves represent the best fit of these experimental points to the simple quadratic equation $K = ad^2 + bd + c$ (*d*: interadduct distance; *a*–*c*: constants).[61]

As oxaliplatin and its *S*,*S* enantiomer exhibit antitumor activity different from that of cisplatin and as we found considerable differences in the DNA conformation distorted by the interstrand CLs of $[Pt(R,R\text{-dach})]^{2+}$, $[Pt(S,S\text{-dach})]^{2+}$, and cisplatin, it was also of considerable interest to examine whether the interstrand CLs of these complexes are recognized differently by HMG domain proteins. The interactions of the domains A and B of the HMGB1 protein, which is the prototypical member of the family of these proteins, with 1,2-GG interstrand CLs of $[Pt(R,R\text{-dach})]^{2+}$ or $[Pt(S,S\text{-dach})]^{2+}$ were investigated by gel mobility shift experiments.[32,41] In these experiments, the 22-bp duplex with blunt ends (see Figure 7C for its sequence) was modified so that it contained a single, site-specific interstrand CL formed by $[Pt(R,R\text{-dach})]^{2+}$, $[Pt(S,S\text{-dach})]^{2+}$, or cisplatin between G residues in the central 5′-GC/5′-GC sequence. For comparative purposes, the 22-bp duplex was also used; this duplex was identical to that containing the interstrand CL except that its central sequence was TGGT/ACCA, at which a single, site-specific 1,2-GG intrastrand CL of cisplatin was formed (Figure 7C). The binding of the domains HMGB1a or HMGB1b to these DNA probes was detected by retardation of the migration of the radiolabeled 22-bp probes on the gel.[40,42,43] These proteins exhibited negligible binding to the unmodified 22-bp duplexes, whereas both HMGB1a and HMGB1b recognized and bound to the duplex containing the 1,2-GG intrastrand CL of cisplatin. HMGB1b also recognized and bound to the duplex containing the interstrand CL of this metallodrug (indicated by the presence of a shifted, more slowly migrating band) in the same way as shown previously, for instance, in our recent papers.[32,41] The results of the titration of the duplexes containing the interstrand CL of $[Pt(R,R\text{-dach})]^{2+}$ or $[Pt(S,S\text{-dach})]^{2+}$ with the domains HMGB1a or HMGB1b indicate that neither of these proteins bound the probes interstrand cross-linked by $[Pt(R,R\text{-dach})]^{2+}$ or $[Pt(S,S\text{-dach})]^{2+}$ under conditions when the HMGB1a or HMGB1b proteins exhibited a considerable affinity for the duplex containing the 1,2-GG intrastrand or interstrand CL of cisplatin, respectively (Figure 7A,B). Hence, the interstrand CLs of $[Pt(R,R\text{-dach})]^{2+}$ or $[Pt(S,S\text{-dach})]^{2+}$ are not recognized by HMG domain proteins or the affinity of these proteins for the interstrand CLs of $[Pt(R,R\text{-dach})]^{2+}$ or $[Pt(S,S\text{-dach})]^{2+}$ is markedly lower than that for the 1,2-GG intrastrand CL and interstrand CL of cisplatin.

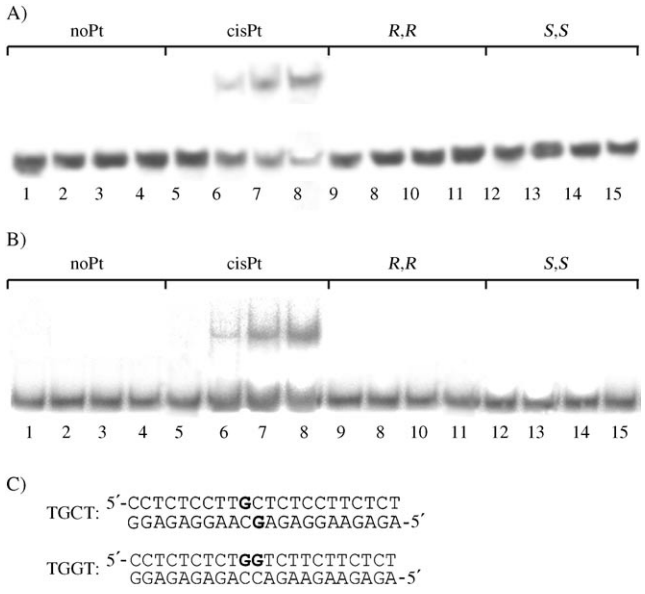

Figure 7. Gel mobility shift assay analysis of the titration of the duplex TGCT (for sequence, see C) containing a single interstrand cross-link of $[Pt(R,R\text{-dach})]^{2+}$ (oxaliplatin) or $[Pt(S,S\text{-dach})]^{2+}$ with HMGB1a (A) and HMGB1b proteins (B). For comparative purposes, gel mobility shift assay analyses of the titration of the duplex TGGT (for sequence, see C) containing a single 1,2-GG intrastrand cross-link of cisplatin with HMGB1a and the duplex TGCT containing an interstrand cross-link of cisplatin with HMGB1b are also shown in A and B, respectively. The concentration of the duplexes was 10 nM. A) Lanes: NoPt: control, nonmodified TGCT duplex; cisPt: the TGGT duplex containing a 1,2-GG intrastrand cross-link of cisplatin; *R*,*R*, *S*,*S*: the TGCT duplex containing an interstrand cross-link of $[Pt(R,R\text{-dach})]^{2+}$ or $[Pt(S,S\text{-dach})]^{2+}$, respectively; lanes 1, 5, 9, and 12: no protein added; lanes 2, 6, 10, and 13: HMGB1a (9.6 nM) added; lanes 3, 7, 11, and 14: HMGB1a (19.2 nM) added; lanes 4, 8, 12, and 15: HMGB1a (38.4 nM) added. B) Lanes: NoPt: control, nonmodified TGCT duplex; cisPt, *R*,*R*, *S*,*S*: the TGCT duplex containing an interstrand cross-link of cisplatin, $[Pt(R,R\text{-dach})]^{2+}$, or $[Pt(S,S\text{-dach})]^{2+}$, respectively; lanes 1, 5, 9, and 12: no protein added; lanes 2, 6, 10, and 13: HMGB1b (4.7 μM) added; lanes 3, 7, 11, and 14: HMGB1b (9.4 μM) added; lanes 4, 8, 12, and 15: HMGB1b (18.8 μM) added. C) Sequences and abbreviations of the synthetic oligodeoxyribonucleotide duplexes used in the gel mobility shift assay. The boldface letters indicate the platinated residues in the cross-linked duplexes.

Discussion

The goal of this study was to probe the hypothesis that differences in the biological effects of oxaliplatin and cisplatin (including cytotoxicity) might possibly result from differences in the character and processing of highly lethal lesions formed by these metallodrugs, such as DNA interstrand CLs. In the present work, data characterizing interstrand CLs of oxaliplatin and its *S*,*S* enantiomer $[Pt(S,S\text{-dach})]^{2+}$, obtained by various biochemical methods currently used for the analysis of DNA distortions induced by DNA-damaging agents, are reported for the first time and some of these characteristics are summarized in Table 2. The DACH ligand is chiral and oxaliplatin exhibits higher activity toward various cancer cell lines than the *S*,*S* enantiomer, so oxaliplatin, and not its *S*,*S* enantiomer, has been approved for clinical use.[44] Although the asymmetry in the amine ligand in the DACH platinum complexes does not involve the coordinated nitrogen atoms but rather the adjacent carbon atoms, a dependence of the biological activity upon the configuration of the amine is observed. Hence, it was also of great interest to answer the question of whether the character of the conformational distortions induced in DNA by interstrand CLs of $[Pt(dach)]^{2+}$ complexes is chirality dependent and different from those of the parent cisplatin.

The CD spectra of duplexes containing single, site-specific interstrand CLs of $[Pt(R,R\text{-dach})]^{2+}$ or $[Pt(S,S\text{-dach})]^{2+}$

(Figure 4A) confirm that the CLs of these two platinum complexes considerably alter the global geometry of the parent duplex. It has been shown[29,31,45] that the cisplatin interstrand CL, which is preferentially formed between opposite guanines in the 5′-GC/5′-GC sequence,[13] induces several irregularities at the cross-linked base pairs in a base-sequence-independent manner.[28] We found that $[Pt(dach)]^{2+}$ complexes also form interstrand CLs at the same sites (Figure 2A) and with the same frequency (Figure 1) as the parent cisplatin, so similar conformational features, although quantitatively different, may be also expected for the interstrand CLs of $[Pt(dach)]^{2+}$ compounds. For instance, the deoxyriboguanosine residues that are interstrand cross-linked by cisplatin are not paired with hydrogen bonds to the complementary deoxyribocytidines, which are located outside the duplex and not stacked with the other aromatic bases; all other base residues are paired.[29,46] Consistent with this characterization is the strong reactivity of chemical probes with cytosine residues complementary to the platinated guanine residues[27] (Figure 5 and Table 2). As the same strong reactivity of chemical probes is also observed in the case of the interstrand CLs of $[Pt(R,R\text{-dach})]^{2+}$ or $[Pt(S,S\text{-dach})]^{2+}$ (Figure 5 and Table 2), it is reasonable to conclude that the interstrand CLs of DACH compounds and cisplatin adopt a similar overall conformation, although some features may be different. Interestingly, chemical probing of the conformational distortions induced in DNA by the interstrand CLs indicates that the distortion induced by the CL of cisplatin is considerably more localized to the platinated base pairs than that induced by the CL of $[Pt(dach)]^{2+}$ complexes. The distortion induced by the interstrand CLs of $[Pt(dach)]^{2+}$ complexes extends over few base pairs flanking the cross-linked base pairs, with the CL of $[Pt(S,S\text{-dach})]^{2+}$ being more efficient in this respect (Figure 5 and Table 2). The severe conformational alteration in the base pairs cross-linked by $[Pt(R,R\text{-dach})]^{2+}$, $[Pt(S,S\text{-dach})]^{2+}$, or cisplatin results in helix unwinding relative to B-DNA by 96, 82, and 79°, respectively (Table 2); this unwinding is very likely responsible for the marked reduction of the amplitude of the negative CD band at around 240 nm (Figure 4A).

Another striking difference between the interstrand CLs of $[Pt(dach)]^{2+}$ complexes and cisplatin is in the ability of the CLs of $[Pt(dach)]^{2+}$ complexes to induce more pronounced bending of the helix axis toward the minor groove at the cross-linked site (Table 2). An important feature of the structure of the interstrand CL of the parent cisplatin is that the platinum residue protrudes into the minor groove of the DNA duplex and the N7 atoms of the cross-linked guanine residues (localized initially in the major groove of B-DNA) move into the minor groove.[29,46] The present work demonstrates that several conformational features of the interstrand CLs of cisplatin and $[Pt(dach)]^{2+}$ compounds, such as bending and unwinding (Table 2), are relatively strong. Hence, this radical distortion of DNA conformation is likely to be associated with the presence of the platinum atom in the minor groove in the interstrand CLs of $[Pt(dach)]^{2+}$ compounds as well. This suggestion is corroborated by the fact that a very high unwinding induced by $[Pt(dach)]^{2+}$ interstrand CLs cannot be rationalized by major-groove models of this lesion.[29] Thus, it seems reasonable to suggest that the bulky DACH group does not restrict the DNA bending required for the formation of the interstrand CL as proposed for bending due to the 1,2-GG intrastrand CL of oxaliplatin.[11]

Formation of the interstrand CLs of $[Pt(dach)]^{2+}$ compounds and cisplatin results in overall thermal stabilization of the duplex (Table 1) and this thermal stabilization is associated mainly with the change in molecularity of the system. On the other hand, we have demonstrated that another important factor affecting the overall thermal stability of the host duplex is the structural perturbation imposed on the duplex by the interstrand CL of the platinum compounds. This conformational distortion thermally destabilizes the host duplex, but this destabilization only partly compensates for the thermal stabilization due to the change in molecularity of the system. We also attempted to rationalize the thermal destabilizing effect of the interstrand CL of $[Pt(dach)]^{2+}$ compounds and cisplatin (Table 2) in terms of the CL-induced structural perturbations in the host duplex. An important feature of the structure of the interstrand CL of cisplatin and presumably also of $[Pt(dach)]^{2+}$ compounds is that cytosine residues complementary to the platinated guanines are no longer hydrogen bonded and are extrahelical (see above). It has been proposed that the hydration of the interstrand CL[45] and the bending induced by the interstrand adducts of cisplatin thermodynamically stabilize the duplex.[47] Although the stabilization resulting from hydration cannot be quantified because of the limited thermodynamic database on DNA hydration, a very crude estimate has been obtained in the case of helical bending. This crude estimation demonstrated that the bending due to the formation of the interstrand CL of cisplatin significantly contributes toward stabilization of the global duplex structure,[47] so it seems reasonable to assume that the contribution of the bending induced by the interstrand CLs of $[Pt(dach)]^{2+}$ compounds is also significant. Another important conformational parameter of the distortion induced by the formation of the interstrand CLs of $[Pt(dach)]^{2+}$ compounds and cisplatin is the unwinding of the double helix (Table 2). The energetics of the destabilizing effect of DNA unwinding due to the interstrand CL of cisplatin were also crudely estimated and it was found that the destabilization of the duplex because of its unwinding as a consequence of the formation of the interstrand CL of cisplatin compensated only partially for the stabilizing effect of the bending.[47] In general, a prediction of the energetic consequences of conformational changes induced by the interstrand CL of $[Pt(dach)]^{2+}$ compounds and cisplatin is difficult because of the limited current knowledge on the thermodynamic consequences of distortions and transitions on DNA duplexes. Nonetheless, the results of the thermal melting experiments reported here reveal that thermal destabilization of the host duplex inversely correlates with the ability of the interstrand CLs of $[Pt(dach)]^{2+}$ compounds and cisplatin to bend the DNA axis (Table 2).

Several proteins that specifically bind to DNA modified by cisplatin, including those containing HMG domains, mediate the antitumor activity of this drug.[3,12] We have found[30,32] that the full-length HMGB1 protein and its domain B with the lysine-rich region of the A/B linker attached to the N terminus do bind to DNA that has been interstrand cross-linked by cisplatin with an affinity similar to that for the major 1,2-GG intrastrand CL of this drug. We demonstrate in the present work that the interstrand CLs of $[Pt(R,R\text{-dach})]^{2+}$ and $[Pt(S,S\text{-dach})]^{2+}$ are not recognized by the HMG domain proteins and that the affinity for these proteins is markedly lower than that of the 1,2-GG intrastrand CL and interstrand CL of cisplatin. Thus, the results of this work can be interpreted to mean that the bulky carrier DACH ligand in $[Pt(R,R\text{-dach})]^{2+}$ and $[Pt(S,S\text{-dach})]^{2+}$ complexes prevents HMG domain proteins from making the contacts with the duplex that are required for recognition and binding of these proteins to the interstrand CLs of $[Pt(dach)]^{2+}$ compounds. Thus, HMG domain proteins discriminate between the interstrand CLs of cisplatin and oxaliplatin, which may be reflected by the differences in the biological effects of these two chemotherapeutic agents.

In summary, this study has allowed us to resolve the effects of the platinum carrier ligand on the structure and other properties of interstrand CLs of oxaliplatin; differences between interstrand CLs of oxaliplatin and cisplatin appear to reflect the effect of the presence of the 1,2-diaminocyclohexane carrier ligand. The interstrand CLs represent less common DNA adducts of mononuclear bifunctional platinum antitumor drugs. Nonetheless, the differences between the properties of the adducts formed by oxaliplatin and cisplatin and in their recognition by HMG domain proteins are remarkably distinct. It is therefore justified to suggest that these differences are at least partly responsible for the differences in the tumor range, toxicity, and mutagenicity of these two chemotherapeutic agents. This suggestion is also reinforced by the fact that, in general, interstrand CLs formed by various compounds of biological significance are more inhibitory to DNA replication and transcription because of the damage sustained by both complementary strands and the resultant severe blockages imposed on DNA-dependent polymerases. In addition, interstrand CLs are more difficult to repair, probably requiring both nucleotide excision and recombinational repair, and thus lead to greater cytotoxicity than that expected for monoadducts or other intrastrand lesions (which can be repaired solely by nucleotide excision).

Experimental Section

Chemicals: $[Pt(R,R\text{-dach})(H_2O)_2](SO_4)$ or $[Pt(S,S\text{-dach})(H_2O)_2](SO_4)$ were prepared from the corresponding dichlorido species[48] by treatment with Ag_2SO_4.[49] Cisplatin was obtained from Sigma (Prague, Czech Republic). The stock solutions of the platinum complexes (5×10^{-4} M in $NaClO_4$ (10 mM)) were stored in the dark at 4°C. Plasmid pSP73KB (2455 bp) was isolated according to standard procedures. Restriction endonuclease *Eco*RI and T7 polynucleotide kinase were purchased from New England Biolabs. The Klenow fragment of DNA polymerase I was from Boehringer-Mannheim Biochemica. The synthetic oligodeoxyribonucleotides were purchased from VBC-genomics (Vienna, Austria) or DNA Technology (Aarhus, Denmark). The purity of oligonucleotides was verified by high-pressure liquid chromatography (HPLC) or gel electrophoresis. Expression and purification of the domains A and B (residues 1–84 and 85–180, respectively) of the HMGB1 protein (HMGB1a and HMGB1b, respectively) were carried out as previously described.[50,51] (Thus, in this work, the HMGB1b protein also contained the A/B linker (residues 85–91) as in our previous work.[32]) T4 DNA ligase and T4 polynucleotide kinase were purchased from New England Biolabs (Beverly, MA). Acrylamide, bis(acrylamide), agarose, and NaCN were from Merck KgaA (Darmstadt, Germany). Dimethyl sulfate (DMS), $KMnO_4$, DEPC, KBr, and $KHSO_5$ were from Sigma (Prague, Czech Republic). [γ-^{32}P]-deoxyriboadenosine triphosphate ([γ-^{32}P]dATP) was from MP Biomedicals, LLC (Irvine, CA).

Platination reactions: The duplex containing a single, site-specific interstrand CL of the platinum compounds was prepared in the following way. The single-stranded oligonucleotides (the top strands of the duplexes used in the present work) were treated with $[Pt(R,R\text{-dach})]^{2+}$, $[Pt(S,S\text{-dach})]^{2+}$, or cisplatin in the dark. The platinated oligonucleotide was repurified by HPLC. It was verified by flameless atomic absorption spectrophotometry (FAAS) and by measurement of the optical density that the modified oligonucleotides contained one molecule of platinum complex per strand. By using Maxam–Gilbert (DMS) footprinting of platinum on DNA,[13,52,53] we also verified that, in the platinated top strands, the N7 atom of a single guanine residue was not accessible for reaction with DMS. The platinated top strands were allowed to anneal with unplatinated complementary strands (the bottom strand of the duplexes shown in Figure 3 B) in $NaClO_4$ (0.1 M) and subsequently incubated at 37°C for 24 h. The resulting products were further characterized as described in the text.

DNA interstrand cross-linking: The 2455-bp double-stranded DNA probe was prepared by digesting the pSP73KB plasmid with *Eco*RI, which cuts only once within this plasmid. The resulting fragment was purified by using the Wizard SV and PCR Clean-Up system and radiolabeled by treatment with the Klenow fragment of DNA polymerase I at 37°C for 1 h in buffer containing NaCl (50 mM), Tris-HCl (10 mM, pH 7.9), $MgCl_2$ (10 mM), 1,4-dithiothreitol (DTT; 1 mM), and [α-^{32}P]dATP (10 μCi, 3000 Ci mmol^{-1}). Unincorporated [α-^{32}P]dATP was removed by a Sephadex G50 column and the DNA was extracted with phenol/chloroform (1:1), precipitated by ethanol and dissolved in $NaClO_4$ (0.1 M). The fragment (0.5 μg) was incubated with the platinum complexes in $NaClO_4$ (0.01 M) at 37°C in the dark for 24 h to attain a value of $r_b = 0.001$. (It was verified, as in our previous papers,[33,54] that under these conditions $[Pt(R,R\text{-dach})]^{2+}$, $[Pt(S,S\text{-dach})]^{2+}$, and cisplatin bound to the DNA quantitatively.) The volume of these reactions was 20 μL. After the incubation, the samples were precipitated by ethanol and the pellet was dissolved in a solution (18 μL) containing NaOH (30 mM), EDTA (1 mM), sucrose (6.6%), and bromophenol blue (0.04%). The amount of interstrand CLs was analyzed by electrophoresis under denaturing conditions on alkaline agarose gel (1.5%). After the electrophoresis was completed, the radioactivity associated with the individual bands in each lane was measured to obtain estimates of the fraction of non-cross-linked or cross-linked DNA under each condition. The frequency of interstrand CLs (% ICL/Pt) was calculated from the fraction of non-cross-linked DNA in combination with the level of platination and the fragment size as $\%\,ICL/Pt = XL/4910\times r_b$, in which XL is the number of interstrand CLs per molecule of the DNA duplex, which was calculated by assuming a Poisson distribution of the interstrand CLs as $XL = -\ln A$, in which A is the fraction of molecules running as a band corresponding to the non-cross-linked DNA.

Hydroxyl radical footprinting of interstrand cross-links: Platinated (or unplatinated) oligodeoxyribonucleotide duplexes (at a concentration of 6 nM) that had either the top or bottom strand ^{32}P-labeled at the 5′ end were dissolved in a medium of NaCl (50 mM) and Tris-HCl (10 mM, pH 7.5). The cleavage of the phosphodiesteric bonds was performed by incubating the duplexes in $[Fe(NH_4)_2(SO_4)_2]$ (0.04 mM), EDTA

(0.08 mM), H_2O_2 (0.03%), and sodium ascorbate (2 mM) for 5 min at 20°C. The reaction was stopped by adding thiourea (15 mM), EDTA (3 mM), sodium acetate (0.3 M), and *t*RNA (0.3 mg mL^{-1}). After precipitation, the samples were loaded onto a 24% denaturing PAA/8 M urea gel. Maxam–Gilbert sequencing reactions were run in parallel.

UV absorption spectrophotometry: UV absorbance measurements were conducted on a Varian Cary 4000 UV/Vis spectrophotometer equipped with a thermoelectrically controlled cell holder and quartz cells with a pathlength of 1 cm. Absorbance versus temperature profiles were measured at 260 nm. The temperature was raised with a linear heating rate of 0.6°C min^{-1}. For each optically detected transition, the T_m value was determined as previously described.[55] The final absorbance versus temperature profile of each duplex was determined as an average of three independent measurements. The DNA solutions contained Tris-HCl (10 mM, pH 7.2), NaCl (0.1 M), and EDTA (0.1 mM).

Circular dichroism (CD) spectrophotometry: CD spectra were recorded by using a Jasco J-720 spectropolarimeter equipped with a thermoelectrically controlled cell holder. The cell pathlength was 1 cm. Isothermal CD spectra were recorded in the range 220–320 nm in 1 nm increments with an averaging time of 5 s. The DNA concentration was 2 μM for the duplex and the buffer comprised Tris-HCl (10 mM, pH 7.2), NaCl (0.1 M), and EDTA (0.1 mM). The precise sample concentrations were determined from their absorption at 260 nm measured at 90°C in the same buffer by using molar extinction coefficients calculated according to Gray et al.[56] CD was expressed as the difference in the molar absorption of the right-handed and left-handed circularly polarized light, $\Delta\varepsilon$, in units of M^{-1} cm^{-1}, with the molarity being related to the duplex.

Chemical probing of the DNA conformation: The modification of the platinated oligonucleotide duplexes by $KMnO_4$, DEPC, and $KBr/KHSO_5$ was performed as described previously.[21–24] The top or bottom strands of the oligonucleotide duplexes were 5′-end labeled with [γ-^{32}P]ATP and T4 polynucleotide kinase. In the case of the platinated oligonucleotides, platinum was removed after reaction of the DNA with the probe by incubation with NaCN (0.2 M, pH 11) at 45°C for 16 h in the dark.

Ligation and electrophoresis of oligonucleotides: Unplatinated or interstrand-cross-linked 21–25-bp duplexes (shown in Figure 3B as TGCT(21–25)) were 5′-end labeled with [γ-^{32}P]dATP by using T4 polynucleotide kinase. The duplexes were allowed to react with T4 DNA ligase. The resulting samples were subsequently examined on 8% native PAA (mono/bis(acrylamide) ratio of 29:1) electrophoresis gels. Other details of these experiments were as described in previous papers[28,57–59] or as described in the text.

Electrophoretic mobility shift assays with HMGB1 domain proteins: Radioactively labeled 22-bp DNA probes with blunt ends (their sequence is shown in Figure 7C) were titrated with HMGB1a or HMGB1b proteins. The duplexes (10 nM) were titrated with the proteins in 10-μL sample volumes in buffer composed of 2-[4-(2-hydroxyethyl)-1-piperazinyl]ethanesulfonic acid (HEPES; 10 mM, pH 7.5), $MgCl_2$ (10 mM), LiCl (50 mM), NaCl (0.1 M), spermidine (1 mM), bovine serum albumin (0.2 mg mL^{-1}), and Nonidet P40 (0.05% v/v). For all gel mobility shift experiments, samples were incubated on ice for 1 h and made 7% in sucrose and 0.017% in xylene cyanol before loading on running, precooled (4°C), prerun (300 V, 1–2 h) 5% native PAA gels (29:1 acrylamide/bisacrylamide, 0.5× Tris/borate/EDTA buffer comprising Tris-HCl (45 mM), boric acid (45 mM), and EDTA (1 mM, pH 8.3)). Gels were electrophoresed at 4°C and 300 V for approximately 1.5 h, dried, exposed to a molecular imaging plate, and analyzed on a Fujifilm bioimaging analyzer. The radioactivities associated with bands were quantitated with AIDA image analyzer software (Raytest, Germany). Other details have been published previously.[32,43,60]

Other physical methods: FAAS measurements were carried out with a Varian AA240Z Zeeman atomic absorption spectrometer equipped with a GTA 120 graphite tube atomizer. For FAAS analysis, DNA was precipitated with ethanol and dissolved in HCl (0.1 M). The gels were visualized by using the BAS 2500 Fujufilm bioimaging analyzer and the radioactivities associated with bands were quantitated with AIDA image analyzer software.

Acknowledgements

This research was supported by the Grant Agency of the Czech Republic (grant no.: 305/05/2030), the Grant Agency of the Ministry of Health of the Czech Republic (grant no.: NR8562-4/2005), the Ministry of Education of the Czech Republic (grant no.: MSMT LC06030), the Academy of Sciences of the Czech Republic (grant nos.: 1QS500040581 and KAN200200651), and the University of Bari. J.K. is an international research scholar of the Howard Hughes Medical Institute. The authors also acknowledge that their participation in the EU COST Actions D39 enabled them to exchange regularly the most recent ideas in the field of platinum anticancer drugs with several European colleagues.

[1] L. Kelland, *Nat. Rev. Cancer* **2007**, *7*, 573–584.
[2] V. Brabec, V. Kleinwächter, J. L. Butour, N. P. Johnson, *Biophys. Chem.* **1990**, *35*, 129–141.
[3] V. Brabec, *Prog. Nucleic Acid Res. Mol. Biol.* **2002**, *71*, 1–68.
[4] M. M. Jennerwein, A. Eastman, A. Khokhar, *Chem.-Biol. Interact.* **1989**, *70*, 39–50.
[5] J. D. Page, I. Husain, A. Sancar, S. G. Chaney, *Biochemistry* **1990**, *29*, 1016–1024.
[6] J. M. Woynarowski, W. G. Chapman, C. Napier, M. C. S. Herzig, P. Juniewicz, *Mol. Pharmacol.* **1998**, *54*, 770–777.
[7] C. P. Saris, P. J. M. van de Vaart, R. C. Rietbroek, F. A. Blommaert, *Carcinogenesis* **1996**, *17*, 2763–2769.
[8] J. M. Woynarowski, S. Faivre, M. C. S. Herzig, B. Arnett, W. G. Chapman, A. V. Trevino, E. Raymond, S. G. Chaney, A. Vaisman, M. Varchenko, P. E. Juniewicz, *Mol. Pharmacol.* **2000**, *58*, 920–927.
[9] B. Spingler, D. A. Whittington, S. J. Lippard, *Inorg. Chem.* **2001**, *40*, 5596–5602.
[10] Y. Wu, P. Pradhan, J. Havener, G. Boysen, J. A. Swenberg, S. L. Campbell, S. G. Chaney, *J. Mol. Biol.* **2004**, *341*, 1251–1269.
[11] Y. Wu, D. Bhattacharyya, C. L. King, I. Baskerville-Abraham, S.-H. Huh, G. Boysen, J. A. Swenberg, B. Temple, S. L. Campbell, S. G. Chaney, *Biochemistry* **2007**, *46*, 6477–6487.
[12] M. Kartalou, J. M. Essigmann, *Mutat. Res.* **2001**, *478*, 1–21.
[13] M. A. Lemaire, A. Schwartz, A. R. Rahmouni, M. Leng, *Proc. Natl. Acad. Sci. USA* **1991**, *88*, 1982–1985.
[14] D. P. Bancroft, C. A. Lepre, S. J. Lippard, *J. Am. Chem. Soc.* **1990**, *112*, 6860–6871.
[15] M. Leng, D. Locker, M. J. Giraud-Panis, A. Schwartz, F. P. Intini, G. Natile, C. Pisano, A. Boccarelli, D. Giordano, M. Coluccia, *Mol. Pharmacol.* **2000**, *58*, 1525–1535.
[16] J. Kasparkova, O. Novakova, V. Marini, Y. Najajreh, D. Gibson, J.-M. Perez, V. Brabec, *J. Biol. Chem.* **2003**, *278*, 47516–47525.
[17] D. Erie, N. Sinha, W. Olson, R. Jones, K. Breslauer, *Biochemistry* **1987**, *26*, 7150–7159.
[18] C. Hofr, V. Brabec, *Biopolymers* **2005**, *77*, 222–229.
[19] S. E. Osborne, J. Völker, S. Y. Stevens, K. J. Breslauer, G. D. Glick, *J. Am. Chem. Soc.* **1996**, *118*, 11993–12003.
[20] P. E. Nielsen, *J. Mol. Recognit.* **1990**, *3*, 1–24.
[21] V. Brabec, M. Sip, M. Leng, *Biochemistry* **1993**, *32*, 11676–11681.
[22] C. Bailly, D. Gentle, F. Hamy, M. Purcell, M. J. Waring, *Biochem. J.* **1994**, *300*, 165–173.
[23] S. A. Ross, C. J. Burrows, *Nucleic Acids Res.* **1996**, *24*, 5062–5063.
[24] C. Bailly, M. J. Waring in *Diethylpyrocarbonate and osmium tetroxide as probes for drug-induced changes in DNA conformation in vitro* (Ed.: K. R. Fox), Humana Press, Totowa, **1997**, pp. 51–79.
[25] J. Zehnulova, J. Kasparkova, N. Farrell, V. Brabec, *J. Biol. Chem.* **2001**, *276*, 22191–22199.
[26] J. Kasparkova, J. Zehnulova, N. Farrell, V. Brabec, *J. Biol. Chem.* **2002**, *277*, 48076–48086.
[27] M. Sip, A. Schwartz, F. Vovelle, M. Ptak, M. Leng, *Biochemistry* **1992**, *31*, 2508–2513.
[28] J. M. Malinge, C. Perez, M. Leng, *Nucleic Acids Res.* **1994**, *22*, 3834–3839.
[29] H. F. Huang, L. M. Zhu, B. R. Reid, G. P. Drobny, P. B. Hopkins, *Science* **1995**, *270*, 1842–1845.

[30] J. Kasparkova, V. Brabec, *Biochemistry* **1995**, *34*, 12379–12387.
[31] V. Brabec in *Chemistry and structural biology of 1,2-interstrand adducts of cisplatin* (Eds.: L. R. Kelland, N. P. Farrell), Humana Press, Totowa, **2000**, pp. 37–61.
[32] J. Kasparkova, O. Delalande, M. Stros, M. A. Elizondo-Riojas, M. Vojtiskova, J. Kozelka, V. Brabec, *Biochemistry* **2003**, *42*, 1234–1244.
[33] J. Malina, C. Hofr, L. Maresca, G. Natile, V. Brabec, *Biophys. J.* **2000**, *78*, 2008–2021.
[34] J. Kasparkova, O. Novakova, N. Farrell, V. Brabec, *Biochemistry* **2003**, *42*, 792–800.
[35] H. Loskotova, V. Brabec, *Eur. J. Biochem.* **1999**, *266*, 392–402.
[36] L. Ulanovsky, M. Bodner, E. N. Trifonov, M. Choder, *Proc. Natl. Acad. Sci. USA* **1986**, *83*, 862–866.
[37] J. A. Rice, D. M. Crothers, A. L. Pinto, S. J. Lippard, *Proc. Natl. Acad. Sci. USA* **1988**, *85*, 4158–4161.
[38] J. Zlatanova, J. Yaneva, S. H. Leuba, *FASEB J.* **1998**, *12*, 791–799.
[39] E. R. Jamieson, S. J. Lippard, *Chem. Rev.* **1999**, *99*, 2467–2498.
[40] U. M. Ohndorf, M. A. Rould, Q. He, C. O. Pabo, S. J. Lippard, *Nature* **1999**, *399*, 708–712.
[41] J. Kasparkova, O. Novakova, O. Vrana, F. Intini, G. Natile, V. Brabec, *Mol. Pharmacol.* **2006**, *70*, 1708–1719.
[42] S. M. Cohen, Y. Mikata, Q. He, S. J. Lippard, *Biochemistry* **2000**, *39*, 11771–11776.
[43] Q. He, U.-A. Ohndorf, S. J. Lippard, *Biochemistry* **2000**, *39*, 14426–14435.
[44] J. L. Misset, *Brit. J. Cancer* **1998**, *77*, 4–7, Suppl. 4.
[45] F. Coste, J. M. Malinge, L. Serre, W. Shepard, M. Roth, M. Leng, C. Zelwer, *Nucleic Acids Res.* **1999**, *27*, 1837–1846.
[46] F. Paquet, C. Perez, M. Leng, G. Lancelot, J. M. Malinge, *J. Biomol. Struct. Dyn.* **1996**, *14*, 67–77.
[47] C. Hofr, V. Brabec, *J. Biol. Chem.* **2001**, *276*, 9655–9661.
[48] F. P. Fanizzi, F. P. Intini, L. Maresca, G. Natile, R. Quaranata, M. Coluccia, L. Di Bari, D. Giordano, M. A. Mariggio, *Inorg. Chim. Acta* **1987**, *137*, 45–51.
[49] M. Benedetti, L. G. Marzilli, G. Natile, *Chem. Eur. J.* **2005**, *11*, 5302–5310.
[50] M. Stros, *J. Biol. Chem.* **1998**, *273*, 10355–10361.
[51] M. Stros, *Biochemistry* **2001**, *40*, 4769–4779.
[52] V. Brabec, K. Neplechova, J. Kasparkova, N. Farrell, *J. Biol. Inorg. Chem.* **2000**, *5*, 364–368.
[53] V. Brabec, M. Leng, *Proc. Natl. Acad. Sci. USA* **1993**, *90*, 5345–5349.
[54] V. Brabec, J. Kasparkova, O. Vrana, O. Novakova, J. W. Cox, Y. Qu, N. Farrell, *Biochemistry* **1999**, *38*, 6781–6790.
[55] R. Zaludova, V. Kleinwächter, V. Brabec, *Biophys. Chem.* **1996**, *60*, 135–142.
[56] D. M. Gray, S. H. Hung, K. H. Johnson, *Methods Enzymol.* **1995**, *246*, 19–34.
[57] H. S. Koo, H. M. Wu, D. M. Crothers, *Nature* **1986**, *320*, 501–506.
[58] S. F. Bellon, S. J. Lippard, *Biophys. Chem.* **1990**, *35*, 179–188.
[59] J. Kasparkova, N. Farrell, V. Brabec, *J. Biol. Chem.* **2000**, *275*, 15789–15798.
[60] J. Malina, J. Kasparkova, G. Natile, V. Brabec, *Chem. Biol.* **2002**, *9*, 629–638.
[61] S. F. Bellon, J. H. Coleman, S. J. Lippard, *Biochemistry* **1991**, *30*, 8026–8035.

Received: August 28, 2007
Published online: November 19, 2007

